An advance tool to predict ground vibration using effective blast design parameters

Jai Jain[1], Anurag Agrawal[2] and Bhanwar Singh Choudhary[2,*]

[1]Coal India Limited, Northern Coalfields Limited, Singrauli 826 004, India
[2]Mining Engineering Department, Indian Institute of Technology, Dhanbad 826 004, India

The blasting technique is mainly used for breaking the rock mass. It is also required to control blast-induced ground vibrations for the safety of nearby habitats. This study was conducted in two different mines and 56 blast vibration data were collected from overburden benches. During trial blasts, it was confirmed that the study benches had similar geology. Analysis of blasts data was done using advanced data analysis software such as MATLAB-based artificial neural network (ANN) and Waikato Environment for Knowledge analysis (WEKA) and compared with the empirical equations. The ANN prediction model gave a significantly high $R^2 = 0.92$ with a low root mean square error (RMSE, 0.67), while WEKA gave a comparatively low $R^2 = 0.86$ with a high RMSE (1.11).

Keywords: Artificial neural network, blast design parameters, empirical equations, ground vibration, statistical analysis.

THE combination of drilling and blasting is cost-effective in civil construction and rock excavation in mining. The blast nuisances, such as ground vibration, air blasts, fly rocks, back breaks and air overpressure are unavoidable, but can be certainly minimized up to permissible levels[1]. With the optimization of fragmentation, ground vibration is considered to be one of the most critical environmental effects[2]. As a result of research on blasting vibration velocity, seismic peak particle velocity (PPV) is often used as a safety criterion to assess blasting vibration-associated damages[3]. Researchers have proposed several vibration prediction equations. PPV is determined mainly by the maximum charge per hole and the distance between the blast face and the monitoring point[4]. Agrawal *et al.*[5] found that explosive energy utilization is very low during blasting and that the percentage of explosive energy converted into seismic energy is about 3%–20%, which is highly dangerous for nearby structures. If ground vibration is higher than the permissible limits, it is a matter of concern and must be controlled. Currently, the maximum charge per delay is restricted for controlling ground vibration. However, in reality, a large number of variables influence ground vibration.

This study considers the effective blast design parameters to predict PPV using artificial intelligence tools and empirical equations. The tools helped predict PPV with minimum errors. In this study, several empirical equations have been used to predict PPV and make a comparison with other modern tools such as Artificial Neural Network (ANN) and Waikato Environment for Knowledge Analysis (WEKA).

Materials and methods

This study was conducted at the overburdened benches of two open-cast coal mines (mines A and B). These mines are located in the eastern part of Jharia Coalfield, Bharat Coking Coal Limited (BCCL), Jharkhand, India. The mines are being worked by mechanized drilling and blasting with 5–7 m high benches and bench angles close to 80°–85°. Crawler-mounted Down the Hole (DTH) drills of 160 mm are used to drill blast holes. It was found that the powder factor varied between 0.9 and 1.0 m^3/kg at mine A and was 1.8 m^3/kg at mine B. The number of blast holes per round varied from 11 to 52.

The blasting area and vibration-monitoring points were both at the same elevation. The monitoring points and blasting patches were separated by 67–296 m. A seismograph (Mini-Seis) with a geophone for ground vibration and a microphone for air-overpressure measurement was used to monitor blasting vibrations. It was ensured that vibration sensors were plastered to the intact surface of the rock. The location of the monitoring points was adjusted appropriately to ensure the accuracy of the measurements. Figure 1 shows a view of the mines, measuring point, designed blast hole section and blast firing pattern.

Artificial neural network

ANN is an intelligence technique used to solve complex problems. The neural network can be studied from the acquainted pattern. This pattern is trained with an adequate number of sample datasets. The prediction of ANN is based on previous learning, where the output is related to new input datasets of similar pattern[6].

ANN is a computing model with layers of connected nodes that resemble the networked structure of neurons in the brain. Data are used to identify patterns, categorize data

*For correspondence. (e-mail: bhanwarschoudhary@iitism.ac.in)
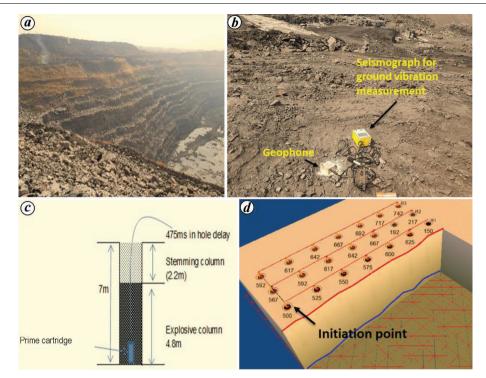
Figure 1. (*a*) Mine view of eastern Jharia coalfield, (*b*) blast monitoring point, (*c*) blast hole section and (*d*) blast firing pattern (diagonal).

Table 1. Prediction of ground vibration using empirical predictors

Model no.	Predictor equations	Reference
1	$\mathrm{PPV} = k\left[\dfrac{R}{\sqrt{Q_{\max}}}\right]^{-\beta}$	17
2	$\mathrm{PPV} = k\left[\dfrac{\sqrt{Q_{\max}}}{R^{2/3}}\right]^{\beta}$	18
3	$\mathrm{PPV} = k\left[\dfrac{R}{\sqrt[3]{Q_{\max}}}\right]^{-\beta}$	19
4	$\mathrm{PPV} = k\left[\dfrac{Q_{\max}}{R^{2/3}}\right]^{\beta}$	20

and predict future events using ANNs. The input is broken down into layers of abstraction by a neural network. This network can be trained over many examples to recognize patterns. By connecting its elements by strength or weight, it defines its function. A specified learning rule adjusts these weights during training until the neural network completes the required task.

Waikato environment of knowledge analysis

In data mining and machine learning, WEKA is an important system[7]. It was developed in response to the perceived need for a unified workspace where researchers could easily access state-of-the-art machine-learning techniques[8]. It consists of data-mining algorithms for machine learning. Java code can call the algorithm directly on a dataset or direct it to the dataset itself. There are many features in WEKA, including pre-processing, classification, regression, clustering, association rules and visualization.

Data preparation results in a dataset with X_1, X_2, X_3, X_n and Y attributes for each record. We aim to derive a function $f: (X_1, \ldots, X_n) \rightarrow Y$ and then use this function to predict Y for a given input record $(x_1, \ldots, x_n)$. In this classification: Y is a discrete attribute, called the class label whether prediction: Y is a continuous attribute. Classification is called supervized learning because true labels (Y-values) are known for the initially provided data.

Empirical equations

Since the 1950s, several empirical equations have been proposed to describe blast vibration attenuation. Table 1 summarizes the PPV prediction equations proposed by different researchers. The distance from the free face and maximum charge weight per delay is usually considered for PPV prediction. The predictor equations are derived from PPV and scaled distance regression analysis. In the equation for vibration propagation, k and β are empirical constants, where k is PPV at the y-axis intercept and β is the slope of the curve. Researchers refer to these empirical constants as site factors, site constants or site-specific constants[9–11].

The strategies to each variable impacts the ground vibration were developed and optimized the blast design considering

Table 2. Summary of blast parameters monitored at mines A and B

Mine A							Mine B						
Input						Output	Input						Output
B (m)	S (m)	MCPD (kg)	TCPD (kg)	R (m)	S/B	PPV (mm/s)	B (m)	S (m)	MCPD (kg)	TCPD (kg)	R (m)	S/B	PPV (mm/s)
2	2.6	35	910	94	1.3	6.15	3.5	4	65	1400	82	1.14	10.7
2	2.6	35	910	85	1.3	10.8	3.5	4	65	1400	115	1.14	5.21
2	2.6	35	910	153	1.3	2.79	3.2	3.5	37	1147	197	1.09	2.26
2	2.5	35	770	87	1.25	9.85	3.2	3.5	37	1147	177	1.09	1.74
2	2.5	35	770	119	1.25	8.33	3.2	3.5	37	1147	97	1.09	8.38
2	2.5	35	770	67	1.25	19.8	3.2	3.5	37	1221	198	1.09	1.98
2	2.5	35	760	127	1.25	1.98	3.2	3.5	37	1221	155	1.09	2.25
2	2.5	35	760	102	1.25	1.65	3.2	3.5	37	1221	108	1.09	6.35
2.5	3	40	1040	115	1.2	5.66	3.2	3.5	37	1332	200	1.09	1.82
2	2.5	25	440	287	1.25	0.91	3.2	3.5	37	1332	195	1.09	1.12
2	2.5	25	440	173	1.25	2.36	3.5	3.8	38.5	1309	163	1.09	3.37
2	2.5	25	440	296	1.25	1.14	3.5	3.8	38.5	1309	201	1.09	3.02
2	2.5	35	500	197	1.25	2.96	3.5	3.8	38.5	1309	148	1.09	2.29
2	2.5	35	500	83	1.25	7.6	3.5	3.5	38.5	963	149	1.00	3.96
2	2.5	35	500	205	1.25	1.65	3.5	3.5	38.5	963	125	1.00	4.64
2	2.5	35	350	204	1.25	0.91	3.5	3.5	38.5	963	126	1.00	3.43
2	2.5	35	350	184	1.25	2.52	3.2	3.5	38.5	1270	166	1.09	3.99
2	2.5	35	350	75	1.25	5.33	3.2	3.5	38.5	1270	214	1.09	1.91
2	2.5	25	310	185	1.25	0.738	3.2	3.5	38.5	1270	150	1.09	2.03
2.5	2.5	35	520	180	1	1.33	3.5	3.5	77	1309	154	1.00	4.51
2.5	2.5	35	520	68	1	9.6	3.5	3.5	77	1309	205	1.00	2.77
2.5	2.5	35	520	227	1	1.52	3.5	3.5	77	1309	156	1.00	2.16
2	3	40	630	126	1.5	3.07	3.5	4	77	1848	160	1.14	3.02
2	3	40	630	102	1.5	3.56	3.5	4	77	1848	141	1.14	3.74
3	3.2	120	1760	147	1.07	9.45	3.5	4	77	1848	114	1.14	6.48
3	3.2	120	1760	249	1.07	3.18	3.2	3.8	77	2002	126	1.19	7.1
2.5	3	80	2040	230	1.2	2.33	3.2	3.8	77	2002	122	1.19	5.98
2.5	3	80	2040	105	1.2	3.18	3.2	3.8	77	2002	107	1.19	11.2

B, Burden; S, Spacing; MCPD, Maximum charge per delay; TCPD, Total charge per delay; R, Radial distance; PPV, Peak particle velocity.
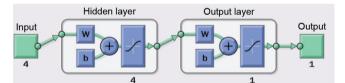

Figure 2. The 4-4-1 architecture of artificial neural network (w and b are weight and biases respectively).

vibration[12]. The particle speed was measured vertically, transversely and longitudinally, and the reported PPV value represents the maximum magnitude of these three components. From the spectrum of the measured vibration, the dominant frequency of the ground vibration signal is calculated. While cracking and structural damage are associated with a wide range of frequencies and amplitudes (PPV), it is generally considered that they depend on ground vibrations[13]. The limitation of ground vibration (PPV) is fixed by the measured dominant frequency at the point of interest.

Summary of monitored blasts and analysis

Table 2 shows the ground vibration monitored at mines A and B.

Analysis of blast vibration using ANN tool

As shown in Figure 2, a feed-forward back-propagation neural network with three layers, namely an input layer, a hidden layer and an output layer, was developed. Due to its ability to handle extensive input data and solve complex problems, this four-layered neural network can predict blast-induced ground vibrations. With regard to 'feed-forward back-propagation', the inputs are activated in a forward direction, while errors in weight adjustment are propagated in the backward direction. In MATLAB, the ANN model was generated as follows: (i) Loading data into the command window. (ii) Establishing a network using 'nntool' function. (iii) Training, validation and testing.

For study investigation, 56 datasets were divided into training datasets (40 data) and testing datasets (16 data). The data were imported into MATLAB using the command window and the network was built with the 'nntool' function. The network window was opened by typing the nntool command in the command window, which allows to import and export of neural networks and data. The feed-forward back-propagation network was chosen for training because it is ideal for nonlinear fits. The Trainlm training function

Table 3. Selection of the number of neurons based on the statistical standard R^2

	Nodes in the hidden layer	Run 1		Run 2	
Model no.		Training	Testing	Training	Testing
1	1	0.727	0.6492	0.692	0.64
2	2	0.512	0.7129	0.543	0.724
3	3	0.744	0.7649	0.74	0.7534
4	4	0.9017	0.92	0.832	0.817
5	5	0.71	0.7865	0.703	0.783
6	6	0.709	0.7126	0.7	0.692
7	7	0.69	0.723	0.72	0.743

Figure 3. Artificial Neural Network analysis of training, testing and validation data.

was selected since it is the quickest back-propagation algorithm in the toolbox. The Trainlm function uses Levenberg–Marquardt optimization to update weight and bias parameters. Since this function requires numerous inputs, the learning functionality used is Learngdm. To build the network, the performance functions such as mean square error (MSE), number of neurons, number of layers and transfer functions, such as tansig were chosen carefully. Following the completion of a network, the next stage was to train the same.

The Levenberg–Marquardt back-propagation algorithm was used to train the network since it is very fast. A set of targets was determined for the provided set of inputs. The network calculates some outputs using transfer functions utilizing random weights (i.e. tansig and logsig). The network error was calculated by comparing the computed results with the predetermined objectives. Validation and testing were done to determine the accuracy of the network. The optimal network architecture was chosen following training, validation and testing with multiple network topologies. For the best model, the number of neurons in the hidden layer was determined by trial and error. Table 3 shows the R^2 values as a function of the number of neurons in the hidden layer.

Figure 3 depicts a regression curve illustrating the link between training, validation and testing outputs and targets. There is an excellent correlation of roughly $R^2 = 0.90$ between the output and target datasets for the training, validation and testing stages.

Table 4 shows how the optimal network was used to forecast 16 new datasets with known outputs. The predicted outcome was then compared with the available results to determine the optimum model accuracy. The observed outputs were compared with the predicted values (Figure 4).

The coefficient of determination (R^2) for Figure 4 is close to 0.92, suggesting that the projected and measured values for the output parameters utilizing the optimal ANN tool are highly correlated. The optimum ANN model predicts the actual physical field behaviour, as evidenced by a strong correlation between the predicted and measured outputs; thus, the ANN model can predict outputs in the field based on known input data.

Data analysis using WEKA

A total of 56 datasets were used for the study. The data were divided into a training dataset and a testing dataset manually. The training dataset contained 40 instances with five attributes, while the testing dataset contained 16 instances with five attributes. The data were loaded either in 'ARFF' format or 'CSV' format. The input parameters used for the experiment were (i) Total charge per round (TC), (ii) distance between the blast sites and the monitoring station (R), (iii) maximum charge per delay (MCPD) and (iv) spacing/burden ratio (S/B). Among several parameters, the four chosen input parameters are known from the literature to significantly influence ground vibration[14,15]. Thus, data analysis was carried out with these four input parameters and one output parameter (PPV) for the 56 different blast datasets. The inputs were enumerated as follows. After loading the data into explorer, they are refined, also known as data cleaning. Figure 5 shows pre-processing of the dataset. Figure 6 shows the relationship between measured PPV and predicted PPV using the WEKA software. The

graph has high coefficient of determination ($R^2 = 0.86$) values, signifying a strong correlation between the predicted and measured output parameters.

Analysis of blast vibration using empirical equations

Various empirical equations were used to predict ground vibration as proposed by several researchers (Table 5). In this analysis, the same data were divided into training and testing. The equations were expressed in linear by a logarithmic transformation of variables. By plotting the graph between log-transformed PPV and the log-transformed

Table 5. Coefficients related to the empirical models used in this study

Predictor equations	k	β
Duvall and Fogelson predictor (1962)	350.83	1.50
Langefors and Kihlstrom predictor (1963)	2.02	2.49
Ambraseys–Hendron predictor (1968)	1207.7	1.59
Indian Standard predictor (1973)	2.067	1.24

Table 4. Measured and predicted PPV

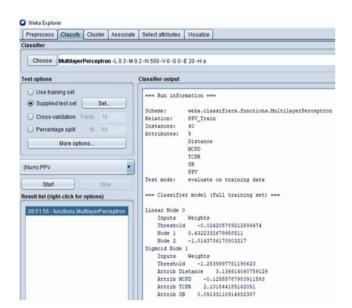| Measured PPV (mm/s)	Predicted PPV (mm/s)
2.29	3.48
3.96	3.56
4.64	4.86
3.43	4.78
3.99	3.73
1.91	1.67
2.03	3.37
4.51	4.06
2.77	1.77
2.16	2.34
3.02	3.14
3.74	3.8
6.48	6.06
7.1	6.98
5.98	5.9
11.2	10.90

Figure 5. Result window showing WEKA running information.

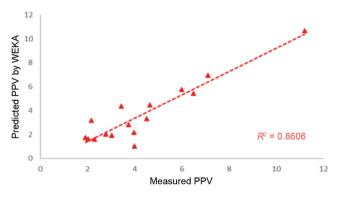**Figure 4.** Relation between predicted and measured peak particle velocity using ANN.
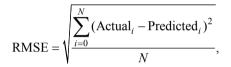

Figure 6. Measured and predicted PPV using WEKA.

scaled distances, the site-specific constants k and β are generated (Table 5). Figure 7 shows the correlation between PPV and scaled distance.

Using empirical predictors, Figure 8 establishes the relationship between measured and predicted PPVs. On the other hand, the trend lines have low R^2 values, indicating a weak relationship between measured and predicted PPVs. The lack of a good relationship is due to the inability of the empirical equations to account for the inherent complexities in the input parameters, necessitating the use of the ANN model.

Results and discussion

Table 6 summarizes R^2 and root mean square error (RMSE) for ANN and various conventional vibration prediction equations. Here, the maximum RMSE obtained by the Ambrasey–Hendron equation predictor is 1.31, which is high compared to both the models (ANN and WEKA).

$$\text{RMSE} = \sqrt{\dfrac{\displaystyle\sum_{i=0}^{N}(\text{Actual}_i - \text{Predicted}_i)^2}{N}},$$

where Predicted is the predicted output, Actual is the measured output and N is the number of input–output data pairs.
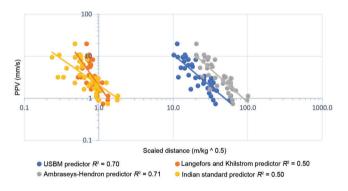

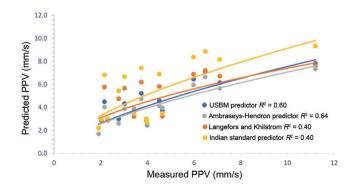**Figure 7.** PPV and scaled distance on log–log scale by predictor equations.

Figure 8. Measured and predicted PPV using predictor equations.

Table 6 shows a higher coefficient of determination (R^2) for the ANN predictor and WEKA model. Compared to the other empirical predictors and the WEKA model, ANN shows the highest coefficient of determination ($R^2 = 0.92$) with low RMSE (0.67). This indicates that ANN is the most suitable tool for predicting PPV.

Statistical analysis

The factorial regression was analysed between design parameters (PPV vs MCPD, TCPD, S/B and R) to examine the effectiveness of the blast designed parameter. Many correlations such as coefficient analysis, normal distribution, interaction plot and Pareto chart analysis[16] were determined between the blast parameters using the mini-tab software. Coefficient analysis was used to analyse the effective parameter ('effect' column) and P-value between the blast parameters in Table 7.

In the factorial regression in Table 7, the parameter R and interaction parameters MCPD∗TCPD∗R show a more significant effect on ground vibration as the P-value is less than 0.1 after considering the 90% confidence level of the interval. Also, the column 'effect' defines the magnitude of the individual and combined effects on the ground vibration (PPV). The combined parameters MCPD∗TCPD∗R show a maximum correlative effect (45.91) on the positive side, while the individual parameters MCPD and R show the maximum effect on the positive (5.22) and negative (–25.18) side respectively, for the ground vibration. Positive and negative define the direct and indirect effects on the output. The results clearly demonstrate the effect of MCPD and radial distance on the ground vibration compared to other parameters. Figure 9 a–c also shows the effective relationship between these parameters.

Figure 9 a shows the normal plot of the standardized effects. In this response analysis, the significant and non-significant parameters can be easily determined. The interaction parameters MCPD, R and TCPD showed about 95% effect on the ground vibration compared to other parameters. Also, the R parameter was effective on the negative side, indicating that with a decrease in R, PPV will increase. The same is the case for the Pareto chart analysis; the interaction parameters MCPD∗TCPD∗R and individual R cross the red dotted line, which is significant at a 95% confidence interval (Figure 9 b). From Figure 9 c, the interaction between all the designed parameters can be easily

Table 6. Results of the statistical and empirical models

Predictors	R^2	RMSE
ANN	0.92	0.67
WEKA	0.86	1.11
USBM	0.60	1.32
Ambrasey–Hendron	0.64	1.31
Langefors–Kihlstrom	0.40	1.81
Indian Standard Predictor	0.40	2.28

Table 7. Coefficient analysis of blast design parameters

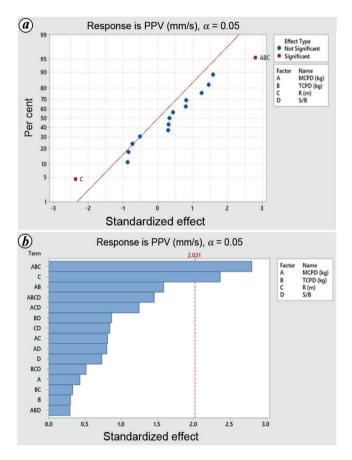| Term	Effect	Coefficient	Standard error (SE) of coefficient	T-value	P-value	Variance inflation factor
Constant		−0.45	3.40	−0.13	0.896	
MCPD (kg)	5.22	2.61	6.03	0.43	0.668	71.72
TCPD (kg)	2.20	1.10	3.64	0.30	0.764	40.83
R (m)	−25.18	−12.59	5.31	−2.37	0.023	54.00
S/B	−5.21	−2.61	3.55	−0.73	0.467	23.86
MCPD (kg)*TCPD (kg)	15.14	7.57	4.77	1.59	0.120	20.68
MCPD (kg)*R (m)	14.64	7.32	8.97	0.82	0.419	94.42
MCPD (kg)*S/B	12.93	6.46	8.06	0.80	0.427	79.46
TCPD (kg)*R (m)	3.74	1.87	5.65	0.33	0.742	33.14
TCPD (kg)*S/B	−11.22	−5.61	6.46	−0.87	0.390	25.57
R (m)*S/B	−13.84	−6.92	8.19	−0.85	0.403	39.44
MCPD (kg)*TCPD (kg)*R (m)	−25.18	22.96	8.18	2.81	0.008	35.87
MCPD (kg)*TCPD (kg)*S/B	4.54	2.27	7.66	0.30	0.768	19.05
MCPD (kg)*R (m)*S/B	36.1	18.1	14.5	1.25	0.219	64.06
TCPD (kg)*R (m)*S/B	−16.0	−8.0	15.4	−0.52	0.606	46.85

Figure 9. *a*, Normal distribution plot of standardized effects. *b*, Pareto chart of the standardized effects. *c*, Interaction plot of the parameters.

determined. The two crossing lines show a strong correlation. The separate line shows no correlation, which demonstrates that the MCPD*R and TCPD*R interaction parameters have more impact on ground vibration. Only two parameters (MCPD and R) have been used to analyse ground vibration in this study.

Conclusion

The present study predicts PPV so that blast impacts can be minimized. The following conclusions can be drawn from the study: (i) ANN is a versatile tool for predicting PPV. High accuracy of prediction and fast computation are the two significant advantages of this method. The ANN model shows a substantial correlation of determination ($R^2 = 0.92$) compared to the other applied models. (ii) In the performance analysis, RMSE of ANN is significantly less (0.67) compared with the other prediction models (WEKA) and four equations (United States Bureau of Mines, Ambrasey, Langefors, Indian Standard). (iii) The Ambrasey–Hendron equation demonstrates a high correlation ($R^2 = 0.71$) compared to other empirical prediction models. (iv) In the statistical analysis, the most significant parameters influencing PPV are MCPD and radial distance, which satisfy the selection of design parameters for ground-vibration analysis.

Conflict of interest: The authors declare that there is no conflict of interest.

1. Choudhary, B. S., Agrawal, A. and Arora, R., Stemming material and Inter-row delay timing effect on blast results in limestone mines. *Sadhana – Acad. Proc. Eng. Sci.*, 2021, **46**, 17–24.
2. Resende, R., Lamas, L., Lemos, J. and Calçada, R., Stress wave propagation test and numerical modelling of an underground complex. *Int. J. Rock Mech. Min. Sci.*, 2014, **72**, 26–36.
3. Yan, W. M., Tham, L. G. and Yuen, K.-V., Reliability of empirical relation on the attenuation of blast-induced vibrations. *Int. J. Rock Mech. Min. Sci.*, 2013, **59**, 160–165.
4. Khandelwal, M. and Singh, T. N., Prediction of blast-induced ground vibration using artificial neural network. *Int. J. Rock Mech. Min. Sci.*, 2009, **46**, 1214–1222.
5. Agrawal, A., Choudhary, B. S. and Murthy, V. M. S. R., Seismic energy prediction to optimize rock fragmentation: a modified approach. *Int. J. Environ. Sci. Technol.*, 2021, **18**, 1–22.
6. Khandelwal, M. and Singh, T. N., Prediction of blast induced ground vibrations and frequency in opencast mine: a neural network approach. *J. Sound Vib.*, 2006, **289**, 711–725.

7. Piatetsky-Shapiro, G., KDnuggets news on SIGKDD service award, 2005; http://www.kdnuggets.com/news

8. Witten, I. H., Frank, E., Hall, M. A., Pal, C. J. and Data, M., Practical machine learning tools and techniques. In *Data Mining*, 2005, p. 4.

9. Khandelwal, M. and Singh, T. N., Evaluation of blast-induced ground vibration predictors. *Soil Dyn. Earthq. Eng.*, 2007, **27**(2), 116–125.

10. Görgülü, K., Arpaz, E., Demirci, A., Koçaslan, A., Dilmaç, M. K. and Yüksek, A. G., Investigation of blast-induced ground vibrations in the Tülü boron open pit mine. *Bull. Eng. Geol. Environ.*, 2013, **72**, 555–564.

11. Rai, R. and Singh, T. N., A new predictor for ground vibration prediction and its comparison with other predictors. *Indian J. Eng. Mater. Sci.*, 2004, **11**, 178–184.

12. Elevli, B. and Arpaz, E., Evaluation of parameters affected on the blast induced ground vibration (BIGV) by using relation diagram method (RDM). *Acta Montan. Slovaca*, 2010, **15**, 261.

13. Dowding, C. H., *Blast Vibration Monitoring and Control*, Prentice-Hall Inc, Englewood's Cliffs, New Jersey, USA, 1985, pp. 288–290.

14. Choudhary, B. S. and Agrawal, A., Blast assessment to improve productivity and safety of habitats in dolomitestone quarry using artificial intelligence. In National Seminar Digitization and e-Governance in Mining Industry, Udaipur, 2019.

15. Bakhsandeh Amnieh, H., Mohammadi, A. and Mozdianfard, M., Predicting peak particle velocity by artificial neural networks and multivariate regression analysis – Sarcheshmeh copper mine, Kerman, Iran. *J. Min. Environ.*, 2013, **4**, 125–132.

16. Radson, D. and Boyd, A. H., The Pareto principle and rate analysis. *Qual. Eng.*, 1997, **10**, 223–229.

17. Duvall, W. I. and Fogelson, D. E., Review of Criteria for Estimating Damage to Residences from Blasting Vibrations. US Department of the Interior, Bureau of Mines, 1962.

18. Langefors, U. and Kihlström, B., *The Modern Technique of Rock Blasting*, Wiley, New York, 1963.

19. Ambraseys, N. R. and Hendron, A. J., Dynamic behavior of rock masses. In *Rock Mechanics in Engineering Practice* (eds Stagg, K. G. and Zienkiewicz, O. C.), John Wiley, London, 1968.

20. Standard, I., Criteria for safety and design of structures subjected to underground blast. ISI, IS-6922, 1973.